

## Mid-rapidity $\phi$ production in Au+Au collisions at $\sqrt{s_{NN}} = 130$ GeV

C. Adler<sup>11</sup>, Z. Ahammed<sup>23</sup>, C. Allgower<sup>12</sup>, J. Amonett<sup>14</sup>, B.D. Anderson<sup>14</sup>, M. Anderson<sup>5</sup>, G.S. Averichev<sup>9</sup>, J. Balewski<sup>12</sup>, O. Barannikova<sup>9,23</sup>, L.S. Barnby<sup>14</sup>, J. Baudot<sup>13</sup>, S. Bekele<sup>20</sup>, V.V. Belaga<sup>9</sup>, R. Bellwied<sup>30</sup>, J. Berger<sup>11</sup>, H. Bichsel<sup>29</sup>, L.C. Bland<sup>12</sup>, C.O. Blyth<sup>3</sup>, B.E. Bonner<sup>24</sup>, R. Bossingham<sup>15</sup>, A. Boucham<sup>26</sup>, A. Brandin<sup>18</sup>, R.V. Cadman<sup>1</sup>, H. Caines<sup>20</sup>, M. Calderón de la Barca Sánchez<sup>31</sup>, A. Cardenas<sup>23</sup>, J. Carroll<sup>15</sup>, J. Castillo<sup>26</sup>, M. Castro<sup>30</sup>, D. Cebra<sup>5</sup>, S. Chattopadhyay<sup>30</sup>, M.L. Chen<sup>2</sup>, Y. Chen<sup>6</sup>, S.P. Chernenko<sup>9</sup>, M. Cherney<sup>8</sup>, A. Chikanian<sup>31</sup>, B. Choi<sup>27</sup>, W. Christie<sup>2</sup>, J.P. Coffin<sup>13</sup>, L. Conin<sup>26</sup>, T.M. Cormier<sup>30</sup>, J.G. Cramer<sup>29</sup>, H.J. Crawford<sup>4</sup>, M. DeMello<sup>24</sup>, W.S. Deng<sup>14</sup>, A.A. Derevschikov<sup>22</sup>, L. Didenko<sup>2</sup>, J.E. Draper<sup>5</sup>, V.B. Dunin<sup>9</sup>, J.C. Dunlop<sup>31</sup>, V. Eckardt<sup>16</sup>, L.G. Efimov<sup>9</sup>, V. Emelianov<sup>18</sup>, J. Engelage<sup>4</sup>, G. Eppley<sup>24</sup>, B. Erasmus<sup>26</sup>, P. Fachini<sup>25</sup>, V. Faine<sup>2</sup>, E. Finch<sup>31</sup>, Y. Fisyak<sup>2</sup>, D. Flierl<sup>11</sup>, K.J. Foley<sup>2</sup>, J. Fu<sup>15</sup>, N. Gagunashvili<sup>9</sup>, J. Gans<sup>31</sup>, L. Gaudichet<sup>26</sup>, M. Germain<sup>13</sup>, F. Geurts<sup>24</sup>, V. Ghazikhanian<sup>6</sup>, J. Grabski<sup>28</sup>, O. Grachov<sup>30</sup>, D. Greiner<sup>15</sup>, V. Grigoriev<sup>18</sup>, M. Guedon<sup>13</sup>, E. Gushin<sup>18</sup>, T.J. Hallman<sup>2</sup>, D. Hardtke<sup>15</sup>, J.W. Harris<sup>31</sup>, M. Heffner<sup>5</sup>, S. Heppelmann<sup>21</sup>, T. Herston<sup>23</sup>, B. Hippolyte<sup>13</sup>, A. Hirsch<sup>23</sup>, E. Hjort<sup>15</sup>, G.W. Hoffmann<sup>27</sup>, M. Horsley<sup>31</sup>, H.Z. Huang<sup>6</sup>, T.J. Humanic<sup>20</sup>, H. Hümmeler<sup>16</sup>, G. Igo<sup>6</sup>, A. Ishihara<sup>27</sup>, Yu.I. Ivanshin<sup>10</sup>, P. Jacobs<sup>15</sup>, W.W. Jacobs<sup>12</sup>, M. Janik<sup>28</sup>, I. Johnson<sup>15</sup>, P.G. Jones<sup>3</sup>, E. Judd<sup>4</sup>, M. Kaneta<sup>15</sup>, M. Kaplan<sup>7</sup>, D. Keane<sup>14</sup>, A. Kisiel<sup>28</sup>, J. Klay<sup>5</sup>, S.R. Klein<sup>15</sup>, A. Klyachko<sup>12</sup>, A.S. Konstantinov<sup>22</sup>, L. Kotchenda<sup>18</sup>, A.D. Kovalenko<sup>9</sup>, M. Kramer<sup>19</sup>, P. Kravtsov<sup>18</sup>, K. Krueger<sup>1</sup>, C. Kuhn<sup>13</sup>, A.I. Kulikov<sup>9</sup>, G.J. Kunde<sup>31</sup>, C.L. Kunz<sup>7</sup>, R.Kh. Kutuev<sup>10</sup>, A.A. Kuznetsov<sup>9</sup>, L. Lakehal-Ayat<sup>26</sup>, J. Lamas-Valverde<sup>24</sup>, M.A.C. Lamont<sup>3</sup>, J.M. Landgraf<sup>2</sup>, S. Lange<sup>11</sup>, C.P. Lansdell<sup>27</sup>, B. Lasiuk<sup>31</sup>, F. Laue<sup>2</sup>, A. Lebedev<sup>2</sup>, T. LeCompte<sup>1</sup>, R. Lednický<sup>9</sup>, V.M. Leontiev<sup>22</sup>, M.J. LeVine<sup>2</sup>, Q. Li<sup>30</sup>, Q. Li<sup>15</sup>, S.J. Lindenbaum<sup>19</sup>, M.A. Lisa<sup>20</sup>, T. Ljubicic<sup>2</sup>, W.J. Llope<sup>24</sup>, G. LoCurto<sup>16</sup>, H. Long<sup>6</sup>, R.S. Longacre<sup>2</sup>, M. Lopez-Noriega<sup>20</sup>, W.A. Love<sup>2</sup>, D. Lynn<sup>2</sup>, R. Majka<sup>31</sup>, S. Margetis<sup>14</sup>, L. Martin<sup>26</sup>, J. Marx<sup>15</sup>, H.S. Matis<sup>15</sup>, Yu.A. Matulenko<sup>22</sup>, T.S. McShane<sup>8</sup>, F. Meissner<sup>15</sup>, Yu. Melnick<sup>22</sup>, A. Meschanin<sup>22</sup>, M. Messer<sup>2</sup>, M.L. Miller<sup>31</sup>, Z. Milosevich<sup>7</sup>, N.G. Minaev<sup>22</sup>, J. Mitchell<sup>24</sup>, V.A. Moiseenko<sup>10</sup>, D. Moltz<sup>15</sup>, C.F. Moore<sup>27</sup>, V. Morozov<sup>15</sup>, M.M. de Moura<sup>30</sup>, M.G. Munhoz<sup>25</sup>, G.S. Mutchler<sup>24</sup>, J.M. Nelson<sup>3</sup>, P. Nevski<sup>2</sup>, V.A. Nikitin<sup>10</sup>, L.V. Nogach<sup>22</sup>, B. Norman<sup>14</sup>, S.B. Nurushev<sup>22</sup>, G. Odyniec<sup>15</sup>, A. Ogawa<sup>21</sup>, V. Okorokov<sup>18</sup>, M. Oldenburg<sup>16</sup>, D. Olson<sup>15</sup>, G. Paic<sup>20</sup>, S.U. Pandey<sup>30</sup>, Y. Panebratsev<sup>9</sup>, S.Y. Panitkin<sup>2</sup>, A.I. Pavlinov<sup>30</sup>, T. Pawlak<sup>28</sup>, V. Perevoztchikov<sup>2</sup>, W. Peryt<sup>28</sup>, V.A. Petrov<sup>10</sup>, W. Pinganaud<sup>26</sup>, E. Platner<sup>24</sup>, J. Pluta<sup>28</sup>, N. Porile<sup>23</sup>, J. Porter<sup>2</sup>, A.M. Poskanzer<sup>15</sup>, E. Potrebenikova<sup>9</sup>, D. Prindle<sup>29</sup>, C. Pruneau<sup>30</sup>, S. Radomski<sup>28</sup>, G. Rai<sup>15</sup>, O. Ravel<sup>26</sup>, R.L. Ray<sup>27</sup>, S.V. Razin<sup>9,12</sup>, D. Reichhold<sup>8</sup>, J.G. Reid<sup>29</sup>, F. Retiere<sup>15</sup>, A. Ridiger<sup>18</sup>, H.G. Ritter<sup>15</sup>, J.B. Roberts<sup>24</sup>, O.V. Rogachevski<sup>9</sup>, J.L. Romero<sup>5</sup>, C. Roy<sup>26</sup>, D. Russ<sup>7</sup>, V. Rykov<sup>30</sup>, I. Sakrejda<sup>15</sup>, J. Sandweiss<sup>31</sup>, A.C. Saulys<sup>2</sup>, I. Savin<sup>10</sup>, J. Schambach<sup>27</sup>, R.P. Scharenberg<sup>23</sup>, K. Schweda<sup>15</sup>, N. Schmitz<sup>16</sup>, L.S. Schroeder<sup>15</sup>, A. Schüttauf<sup>16</sup>, J. Seger<sup>8</sup>, D. Seliverstov<sup>18</sup>, P. Seyboth<sup>16</sup>, E. Shahaliev<sup>9</sup>, K.E. Shestermanov<sup>22</sup>, S.S. Shimanskii<sup>9</sup>, V.S. Shvetcov<sup>10</sup>, G. Skoro<sup>9</sup>, N. Smirnov<sup>31</sup>, R. Snellings<sup>15</sup>, J. Sowinski<sup>12</sup>, H.M. Spinka<sup>1</sup>, B. Srivastava<sup>23</sup>, E.J. Stephenson<sup>12</sup>, R. Stock<sup>11</sup>, A. Stolpovsky<sup>30</sup>, M. Strikhanov<sup>18</sup>, B. Stringfellow<sup>23</sup>, H. Stroebele<sup>11</sup>, C. Struck<sup>11</sup>, A.A.P. Suaide<sup>30</sup>, E. Sugarbaker<sup>20</sup>, C. Suires<sup>13</sup>, M. Šumbera<sup>9</sup>, T.J.M. Symons<sup>15</sup>, A. Szanto de Toledo<sup>25</sup>, P. Szarwas<sup>28</sup>, J. Takahashi<sup>25</sup>, A.H. Tang<sup>14</sup>, J.H. Thomas<sup>15</sup>, V. Tikhomirov<sup>18</sup>, T.A. Trainor<sup>29</sup>, S. Trentalange<sup>6</sup>, M. Tokarev<sup>9</sup>, M.B. Tonjes<sup>17</sup>, V. Trofimov<sup>18</sup>, O. Tsai<sup>6</sup>, K. Turner<sup>2</sup>, T. Ullrich<sup>2</sup>, D.G. Underwood<sup>1</sup>, G. Van Buren<sup>2</sup>, A.M. VanderMolen<sup>17</sup>, A. Vanyashin<sup>15</sup>, I.M. Vasilevski<sup>10</sup>, A.N. Vasiliev<sup>22</sup>, S.E. Vigdor<sup>12</sup>, S.A. Voloshin<sup>30</sup>, F. Wang<sup>23</sup>, H. Ward<sup>27</sup>, J.W. Watson<sup>14</sup>, R. Wells<sup>20</sup>, T. Wenaus<sup>2</sup>, G.D. Westfall<sup>17</sup>, C. Whitten Jr.<sup>6</sup>, H. Wieman<sup>15</sup>, R. Willson<sup>20</sup>, S.W. Wissink<sup>12</sup>, R. Witt<sup>14</sup>, N. Xu<sup>15</sup>, Z. Xu<sup>31</sup>, A.E. Yakutin<sup>22</sup>, E. Yamamoto<sup>6</sup>, J. Yang<sup>6</sup>, P. Yepes<sup>24</sup>, A. Yokosawa<sup>1</sup>, V.I. Yurevich<sup>9</sup>, Y.V. Zanevski<sup>9</sup>, I. Zborovský<sup>9</sup>, W.M. Zhang<sup>14</sup>, R. Zoukarneev<sup>10</sup>, A.N. Zubarev<sup>9</sup>

(STAR Collaboration)

<sup>1</sup>Argonne National Laboratory, Argonne, Illinois 60439,

<sup>2</sup>Brookhaven National Laboratory, Upton, New York 11973,

<sup>3</sup>University of Birmingham, Birmingham, United Kingdom,

<sup>4</sup>University of California, Berkeley, California 94720,

<sup>5</sup>University of California, Davis, California 95616,

<sup>6</sup>University of California, Los Angeles, California 90095,

<sup>7</sup>Carnegie Mellon University, Pittsburgh, Pennsylvania 15213,

<sup>8</sup>Creighton University, Omaha, Nebraska 68178,

<sup>9</sup>Laboratory for High Energy (JINR), Dubna, Russia,

<sup>10</sup>Particle Physics Laboratory (JINR), Dubna, Russia,

- <sup>11</sup>University of Frankfurt, Frankfurt, Germany,  
<sup>12</sup>Indiana University, Bloomington, Indiana 47408,  
<sup>13</sup>Institut de Recherches Subatomiques, Strasbourg, France,  
<sup>14</sup>Kent State University, Kent, Ohio 44242,  
<sup>15</sup>Lawrence Berkeley National Laboratory, Berkeley, California 94720,  
<sup>16</sup>Max-Planck-Institut fuer Physik, Munich, Germany,  
<sup>17</sup>Michigan State University, East Lansing, Michigan 48824,  
<sup>18</sup>Moscow Engineering Physics Institute, Moscow Russia,  
<sup>19</sup>City College of New York, New York City, New York 10031,  
<sup>20</sup>Ohio State University, Columbus, Ohio 43210,  
<sup>21</sup>Pennsylvania State University, University Park, Pennsylvania 16802,  
<sup>22</sup>Institute of High Energy Physics, Protvino, Russia,  
<sup>23</sup>Purdue University, West Lafayette, Indiana 47907,  
<sup>24</sup>Rice University, Houston, Texas 77251,  
<sup>25</sup>Universidade de Sao Paulo, Sao Paulo, Brazil,  
<sup>26</sup>SUBATECH, Nantes, France,  
<sup>27</sup>University of Texas, Austin, Texas 78712,  
<sup>28</sup>Warsaw University of Technology, Warsaw, Poland,  
<sup>29</sup>University of Washington, Seattle, Washington 98195,  
<sup>30</sup>Wayne State University, Detroit, Michigan 48201, and  
<sup>31</sup>Yale University, New Haven, Connecticut 06520

(Dated: August 8, 2001)

We present the first measurement of mid-rapidity vector meson  $\phi$  production in Au+Au collisions at RHIC ( $\sqrt{s_{NN}} = 130$  GeV) from the STAR detector. For the 11% highest multiplicity collisions, the slope parameter from an exponential fit to the transverse mass distribution is  $T = 379 \pm 50(\text{stat}) \pm 45(\text{syst})$  MeV, the yield  $dN/dy = 5.73 \pm 0.37(\text{stat}) \pm 0.69(\text{syst})$  per event and the ratio  $N_{\phi}/N_{h^-}$  is found to be  $0.021 \pm 0.001(\text{stat}) \pm 0.004(\text{syst})$ . The measured ratio  $N_{\phi}/N_{h^-}$  and  $T$  for the  $\phi$  meson at mid-rapidity do not change for the selected multiplicity bins.

PACS numbers: 25.75.Dw

The central topic of relativistic heavy ion physics is the study of Quantum Chromodynamics (QCD) in extreme conditions of high temperature and high energy density over large volumes [1]. Vector mesons may probe the dynamics of particles and chiral symmetry [2] in relativistic heavy ion collisions: their production mechanisms and subsequent dynamical evolution have been a topic of experimental investigation [3–6]. The  $\phi$  meson is of particular interest due to its  $s\bar{s}$  valence quark content, which may make the  $\phi$  sensitive to strangeness production from a possible early partonic phase [7–9].

In central Pb+Pb collisions at SPS (nucleon-nucleon center of mass energy  $\sqrt{s_{NN}} = 17$  GeV), the slope parameter ( $T$ ) in an exponential fit to the transverse mass ( $m_t$ ) distribution at mid-rapidity ( $\propto e^{-m_t/T}$ ) follows a systematic trend as a function of hadron mass for pions, kaons and protons [10]. This observation is indicative of a common expansion velocity developed in the final state for pions, kaons, and protons [11]. However, the slope parameters measured for multi-strange hyperons  $\Xi$  and  $\Omega$  [12], and for  $J/\psi$  [13] show deviations from a linear mass dependence, suggesting that these particles do not interact as strongly in the final state at SPS energies [14]. Measurements of  $\phi$  meson production at the SPS were inconclusive [3, 4]. Largely different values for the  $\phi$  slope parameter have been obtained from exponential fits to the measured  $m_t$  spectra in central Pb+Pb collisions when using the  $K^+K^-$  decay channel [3] and when using the  $\mu^+\mu^-$  decay channel

[4] of the  $\phi$  meson. However, this difference is not apparent in peripheral collisions [15, 16]. Possible scenarios to explain the difference have been discussed in the literature [17, 18].

In this letter, we report the first measurement of mid-rapidity ( $|y| < 0.5$ )  $\phi$  production in Au+Au collisions at RHIC ( $\sqrt{s_{NN}} = 130$  GeV) via the  $\phi \rightarrow K^+K^-$  decay channel (branching ratio = 0.491) using the Solenoidal Tracker At RHIC (STAR) detector [19]. Systematics of  $\phi$  production as a function of centrality at RHIC as well as its  $\sqrt{s_{NN}}$  dependence will be discussed.

The STAR detector consists of several detector sub-systems in a large solenoidal analyzing magnet. For the data taken in the year 2000 and presented here, the experimental setup consisted of a Time Projection Chamber (TPC) [20], a Central Trigger Barrel (CTB), and two Zero Degree Calorimeters (ZDC) located upstream along the beam axis. The TPC is a cylindrical drift chamber with multi-wire proportional chamber readout. With its axis aligned along the beam direction, the TPC provided complete azimuthal coverage. Surrounding the TPC was the CTB, which measured energy deposition from charged particles. The ZDC's measured beam-like neutrons from the fragmentation of colliding nuclei. The CTB was used in conjunction with the ZDC's as the experimental trigger.

Data used in this analysis were taken with two different trigger conditions: a minimum-bias trigger requiring a coincidence between both ZDC's and a central trigger additionally

requiring a high hit multiplicity in the CTB. The central trigger corresponded to approximately the top 15% of the measured cross section for Au+Au collisions. Data from both the minimum-bias trigger and central trigger were used for this analysis.

Reconstruction of the  $\phi$  was accomplished by calculating the invariant mass ( $m_{inv}$ ), transverse momentum ( $p_t$ ), and rapidity ( $y$ ) of all permutations of candidate  $K^+K^-$  pairs. The resulting  $m_{inv}$  distribution consisted of the  $\phi$  signal atop a large background that is predominantly combinatorial. The shape of the combinatorial background was calculated using the mixed-event technique [21, 22].

For the centrality measurement, the raw total charged multiplicity distribution within a pseudo-rapidity window  $|\eta| \leq 0.75$  was divided into three bins corresponding to 85–26%, 26–11% and the top 11% of the measured cross section for Au+Au collisions [23–25]. Events were selected with a primary vertex  $z$  position ( $z$ ) from the center of the TPC of  $|z| < 80$  cm. These events were further divided according to  $z$  in 16 bins, and event mixing was performed for events within each bin to construct background distributions with reduced acceptance-induced distortions in the mixed-event background. Consistent results were obtained when we constructed the background distribution using like-sign pairs from the same event.

Particle identification (PID) was achieved by correlating the ionization energy loss ( $dE/dx$ ) of charged particles in the TPC gas with their measured momentum [25]. By truncating the largest 30%  $dE/dx$  values along the track a sample was selected to calculate the mean  $\langle dE/dx \rangle$ . For the highest multiplicity events, the average  $\langle dE/dx \rangle$  resolution was found to be about 11%. The measured  $\langle dE/dx \rangle$  is reasonably described by the Bethe-Bloch function smeared with a resolution of width  $\sigma$ . Tracks within  $2\sigma$  of the kaon Bethe-Bloch curve were selected for this analysis.

To obtain the  $\phi$  spectra, same event and mixed event distributions were accumulated and background subtraction was done in each  $(m_t, y)$  bin. The mixed event background  $m_{inv}$  distribution was normalized to the same event  $m_{inv}$  distribution in the region above the  $\phi$  mass ( $1.04 < m_{inv} < 1.2$  GeV/ $c^2$ ). A small, smooth residual background can remain near the  $\phi$  peak in the subtracted mass distribution, because the mixed event sample does not properly account for the production of background pairs (kaons and/or pions from PID leak-through) that are correlated, either by Coulomb or other interactions or by such instrumental effects as track merging [26]. The yield in each bin was then determined by fitting the background subtracted  $m_{inv}$  distribution to a Breit-Wigner function plus a linear background in a limited mass range (Figure 1).

Figure 1 (b) shows the  $m_{inv}$  distribution in a relatively high  $p_t$  bin which has a residual background. The magnitude of the residual background is about 1% of the total background before mixed event subtraction. The shape of the residual background is not well constrained by the statistically limited data in this particular bin, but the linear assumption worked well for all momentum bins. The widths of the fits to the invariant

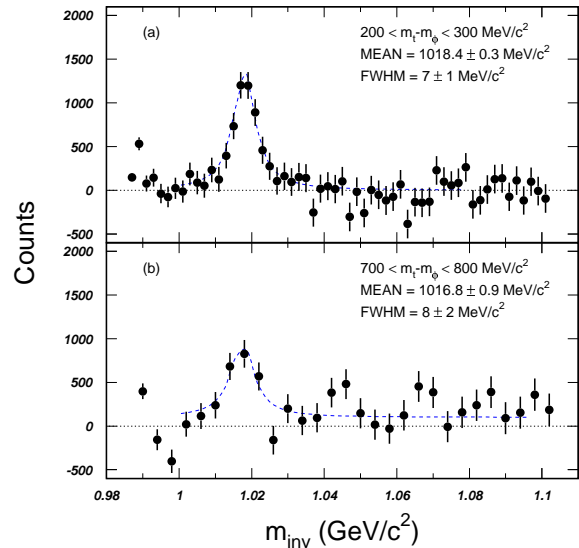


FIG. 1: Invariant mass distributions for candidate  $K^+K^-$  pairs in two  $m_t - m_\phi$  bins after background subtraction for the 11% most central collisions. Bins in panel (a) are  $2$  MeV/ $c^2$  wide while the bins in panel (b) are  $4$  MeV/ $c^2$  wide. The widths of the mass distributions are consistent with the natural width of the  $\phi$  convoluted with the resolution of the TPC. Error bars shown are statistical only.

mass distribution are consistent with the natural width of the  $\phi$  convoluted with the resolution of the TPC. The uncertainties in the extracted  $\phi$  yields are dominated by the statistical errors derived from the fitting procedure, which include the statistical uncertainty from the mixed event background subtraction.

The resulting raw  $\phi$  yield for each  $m_t$ ,  $y$  and multiplicity bin was then corrected for tracking efficiency and acceptance using Monte Carlo simulations of physics processes and detector response. The reconstruction efficiency depended on the  $p_t$  of the  $\phi$ , ranging from  $\sim 10\%$  at  $p_t = 0.46$  GeV/ $c$  up to  $\sim 40\%$  at  $p_t = 1.4$  GeV/ $c$ . The PID efficiency correction for the  $\phi$  was calculated as the square of the single kaon PID efficiency and included the multiplicity dependence of the  $dE/dx$  resolution. The corrected  $\phi$  invariant yields for three event multiplicity bins are shown in Figure 2. All results presented here are for reconstructed  $\phi$  mesons within one unit of rapidity centered around  $y = 0$  ( $|y| < 0.5$ ) and  $0.46 < p_t < 1.74$  GeV/ $c$ . In the region where the pion band crosses the kaon band in  $dE/dx$  [25], corresponding to the kaon  $p_t \simeq 0.8$  GeV/ $c$ , the signal to background ratio degrades. This leads to the larger statistical error bars in the most central bin and prevented the extraction of the  $\phi$  yields in this region for the two lower multiplicity bins. The spectra were fit to an exponential

$$\frac{1}{2\pi m_t} \frac{d^2N}{dm_t dy} = \frac{dN/dy}{2\pi T(m_\phi + T)} e^{-(m_t - m_\phi)/T} \quad (1)$$

with the slope parameter  $T$  and yield  $dN/dy$  set as free param-

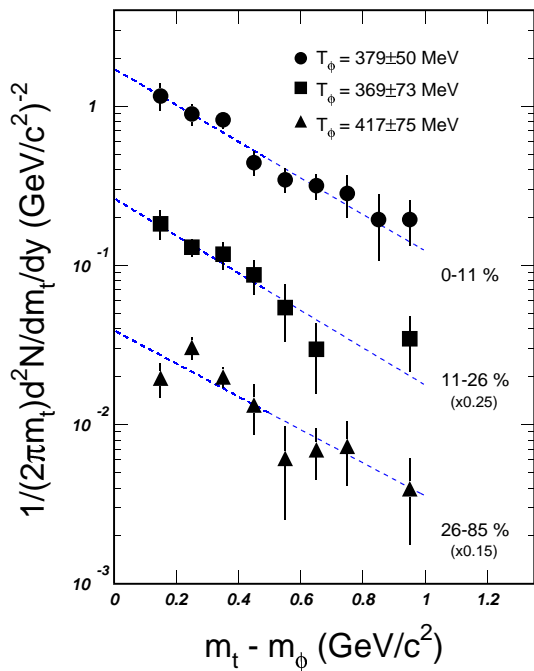


FIG. 2: Transverse mass distributions of  $\phi$  from Au+Au collision at  $\sqrt{s_{NN}} = 130$  GeV for three multiplicity bins. Dashed lines are exponential fits to the data. For clarity, data points from the 11–26% and 26–85% multiplicity bins are scaled by 0.25 and 0.15, respectively. Error bars shown are statistical only.

eters. The obtained results are listed in Table I. The fraction of  $\phi$  mesons in the measured  $p_t$  region assuming an exponential distribution is  $\sim 70\%$ . Also listed is the ratio  $N_\phi/N_{h^-}$  for three multiplicity bins.

The major systematic uncertainties for this analysis include contributions from PID efficiency and tracking efficiency. The systematic error based on different background fits is significantly smaller than the statistical error in all  $p_t$  bins. By varying PID and track quality requirements, we estimate a systematic uncertainty of  $\pm 12\%$  for  $T$ . The total systematic error on  $dN/dy$  is  $\pm 12\%$ , which includes an additional 6% uncertainty (added in quadrature) due to uncertainties in TPC performance. Systematic errors for the ratios also include uncertainties from the  $h^-$  yields. The full range of the systematic uncertainty for  $N_\phi/N_{h^-}$  is  $\pm 22\%$ .

Figure 3 shows a comparison of our results for the  $\phi$  slope parameter to previous measurements at lower collision energies. Filled symbols represent results extracted from approximately the 10% most central heavy ion collisions [3, 6] and the open symbols represent the results from  $p + p$  collisions [3, 27]. For heavy ion collisions, there is an increase in  $T$  from the AGS ( $\sqrt{s_{NN}} \simeq 5$  GeV) to SPS ( $\sqrt{s_{NN}} \simeq 17$  GeV) to RHIC ( $\sqrt{s_{NN}} = 130$  GeV). However, slope parameters from

Event Multiplicity	0–11%	11–26%	26–85%
$T$ (MeV)	$379 \pm 50$	$369 \pm 73$	$417 \pm 75$
$dN/dy$	$5.73 \pm 0.37$	$3.33 \pm 0.38$	$0.98 \pm 0.12$
$N_\phi/N_{h^-}$	$0.021 \pm 0.001$	$0.019 \pm 0.002$	$0.019 \pm 0.002$

TABLE I: Mid-rapidity  $\phi$  slope parameters  $T$ , extrapolated yield  $dN/dy$  and the ratio  $N_\phi/N_{h^-}$  for three multiplicity bins. Errors shown are statistical only.

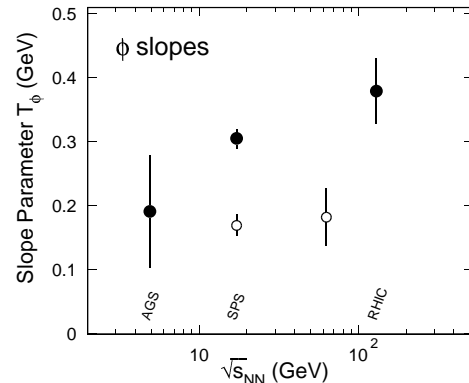


FIG. 3:  $\sqrt{s_{NN}}$  dependence of the mid-rapidity  $\phi$  slope parameter. The data points are from the  $\phi \rightarrow K^+K^-$  decay channel. Filled symbols represent the results extracted from the highest multiplicity heavy ion collisions and the open symbols represent the results from  $p + p$  collisions. Error bars shown are statistical errors only.

$p + p$  collisions show no significant dependence on collision energy up to  $\sqrt{s} = 63$  GeV.

In the highest multiplicity Au+Au collisions at RHIC, the  $\phi$  slope parameter is  $379 \pm 50(\text{stat}) \pm 45(\text{syst})$  and there is no dependence on event multiplicity (Table I) within our statistical uncertainty. However, the anti-proton slope parameter using the same fit function, measured in the  $p_t$  range  $0.25 < p_t < 1$  GeV/c and without correction for feed-down from anti-hyperons, is found to be over 150 MeV higher than the  $\phi$  meson slope measured in  $0.5 < p_t < 1.7$  GeV/c. In addition, the anti-proton slope shows a clear dependence on event multiplicity [25]. Note that if a strong collective flow develops in the system, the measured slope parameter should depend strongly on the fitting range.

The energy dependence of  $N_\phi/N_{h^-}$  is shown in Figure 4. In heavy ion collisions,  $N_\phi/N_{h^-}$  increases with collision energy indicating that  $\phi$  production increases faster than  $h^-$  production up to  $\sqrt{s_{NN}} = 130$  GeV. Although there seems to be a significant increase in  $N_\phi/N_{h^-}$  ratio from  $p + p$  collisions between 17 and 63 GeV [3, 27], the statistical uncertainty in the 63 GeV point is too large to determine the energy dependence. Note that the ratio at Tevatron energies ( $p + \bar{p}$  at  $\sqrt{s} = 1800$  GeV) was found to be about 0.01 [28].

In summary, using the STAR detector we have measured mid-rapidity  $\phi$  production from Au+Au collisions at  $\sqrt{s_{NN}} =$

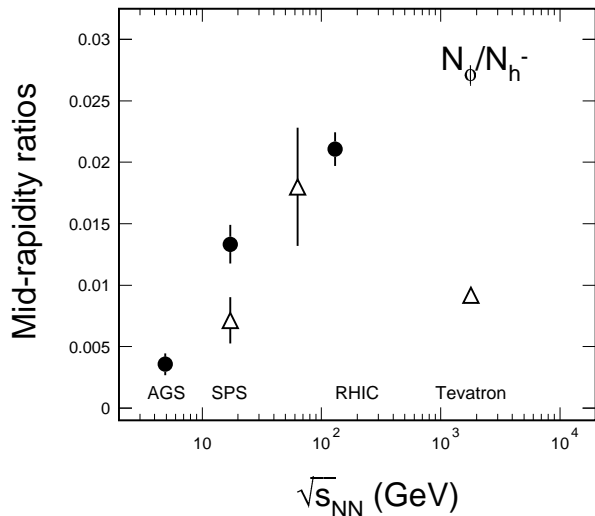


FIG. 4:  $\sqrt{s_{NN}}$  dependence of the mid-rapidity  $N_\phi/N_{h^-}$  ratio. Results were extracted from the  $\phi \rightarrow K^+K^-$  decay channel. Filled symbols represent the results extracted from the highest multiplicity heavy ion collisions and the open symbols represent the results from  $p+p$  (17 and 63 GeV points) and  $p+\bar{p}$  (1800 GeV) collisions. Error bars shown are statistical errors only.

130 GeV. In the most central collisions, the  $\phi$  slope parameter,  $T = 379 \pm 50(\text{stat}) \pm 45(\text{syst})$  MeV, is lower than that of anti-protons in the measured  $p_t$  region. Within statistical uncertainty, there is no variation in  $\phi$  slope parameters and the ratio  $N_\phi/N_{h^-}$  for the selected multiplicity bins. The  $\phi$  slope parameter and the ratio  $N_\phi/N_{h^-}$  increase from  $\sqrt{s_{NN}} \simeq 5$  to 130 GeV.

**Acknowledgments:** We wish to thank the RHIC Operations Group at Brookhaven National Laboratory for their tremendous support and for providing collisions for the experiment. This work was supported by the Division of Nuclear Physics and the Division of High Energy Physics of the Office of Science of the U.S. Department of Energy, the United States National Science Foundation, the Bundesministerium fuer Bildung und Forschung of Germany, the Institut National de la Physique Nucleaire et de la Physique des Particules of France, the United Kingdom Engineering and Physical Sciences Research Council, Fundacao de Amparo a Pesquisa do Estado de Sao Paulo, Brazil, and the Russian Ministry of Science and Technology.

[1] F. Wilczek, *Physics Today*, **53**, Aug. 2000, pg. 22.

[2] T. Hatsuda and T. Kunihiro, *Phys. Rep.* **247**, 221 (1994).

- [3] S.V. Afanasiev *et al.*, NA49 Collaboration, *Phys. Lett.* **B491**, 59 (2000).
- [4] N. Willis *et al.*, NA50 Collaboration, *Nucl. Phys.* **A661**, 534c (1999).
- [5] Y. Akiba *et al.*, E802 Collaboration, *Phys. Rev. Lett.* **76**, 2021 (1996).
- [6] R.K. Seto and H. Xiang, E917 Collaboration, *Nucl. Phys.* **A661**, 506c (1999).
- [7] J. Rafelski and B. Müller, *Phys. Rev. Lett.* **48**, 1066 (1982).
- [8] A. Shor, *Phys. Rev. Lett.* **54**, 1122 (1985).
- [9] P. Koch, B. Müller and J. Rafelski, *Phys. Rep.* **142**, 167 (1986).
- [10] I. Bearden *et al.*, NA44 Collaboration, *Phys. Rev. Lett.* **78**, 2080 (1997).
- [11] U. Heinz, *Nucl. Phys.* **A610**, 264c (1996).
- [12] E. Andersen *et al.*, WA97 Collaboration, *Phys. Lett.* **B433**, 209 (1998).
- [13] M.C. Abreu *et al.*, NA50 Collaboration, *Phys. Lett.* **B499**, 85 (2001).
- [14] H. van Hecke, H. Sorge and N. Xu, *Phys. Rev. Lett.* **81**, 5764 (1998).
- [15] V. Friese *et al.*, NA49 Collaboration, *Quark Matter*, (2001).
- [16] C. Quintans *et al.*, NA50 Collaboration, *J. Phys. G.: Nucl. Part. Phys.* **27**, 405c (2001).
- [17] S. Johnson, B. Jacak and A. Drees, *Eur. Phys. J.* **C18**, 645–649 (2001).
- [18] S. Soff *et al.*, *J. Phys. G.: Nucl. Part. Phys.* **27**, 449c (2001).
- [19] K.H. Ackermann *et al.*, STAR Collaboration, *Nucl. Phys.* **A661**, 681c (1999).
- [20] H. Wieman *et al.*, *IEEE Trans. Nucl. Sci.* **44**, 671 (1997).
- [21] D. L'Hote, *Nucl. Instrum. Meth.* **A337**, 544 (1994).
- [22] D. Drijard, H. G. Fischer and T. Nakada, *Nucl. Instrum. Meth.* **A225**, 367 (1984).
- [23] K.H. Ackermann *et al.*, STAR Collaboration, *Phys. Rev. Lett.* **86**, 402 (2001).
- [24] The measured cross-section is approximately 90% of the total inelastic Au+Au cross-section. Our centrality bins correspond to approximately 77–23%, 23–10% and top 10% of the inelastic Au+Au cross-section.
- [25] J. Harris *et al.*, STAR Collaboration, *Quark Matter*, (2001).
- [26] E. Yamamoto, Ph.D. Thesis, University of California - Los Angeles, (2001).
- [27] T. Åkesson *et al.*, AFS Collaboration, *Nucl. Phys.* **B203**, 27 (1982).
- [28] T. Alexopoulos *et al.*, E735 Collaboration, *Phys. Rev.* **D48**, 984 (1993) and T. Alexopoulos *et al.*, E735 Collaboration, *Z. Phys.* **C67**, 411 (1995).